

Creep-sintering of polycrystalline ceramic particulate composites

R. E. DUTTON, M. N. RAHAMAN

Department of Ceramic Engineering, University of Missouri-Rolla, Rolla, MO 65401, USA

The sintering of particulate composites consisting of a polycrystalline zinc oxide matrix with 10 vol % zirconia inclusions of two different sizes (3 and 14 μm) was investigated at a constant heating rate of 4 $^{\circ}\text{C min}^{-1}$ under an applied stress of ≈ 300 kPa. The presence of the inclusions produced a decrease in both the creep rate and the densification rate but the ratio of the densification to creep rate remained constant during the experiment. The ratio of the densification rate to creep rate for the composites was ≈ 1.5 times greater than that of the unreinforced matrix regardless of inclusion size. The creep viscosity of the composites was higher than that of the unreinforced matrix and increased slightly with decreasing inclusion size.

1. Introduction

It is widely recognized that the presence of inert second-phase particles severely retards the densification rate of polycrystalline matrix composites. While several mechanisms may be operating, the main factors which control the sintering of these composites have been shown to involve (i) the interactions between randomly distributed inclusions which constrain the matrix thereby hindering densification, and (ii) the packing of the matrix phase, especially in the regions immediately surrounding the inclusion [1, 2]. The sinterability of the composites improves with increasing temperature indicating that the constraint produced by the inclusions is increasingly relaxed at higher temperatures [1]. Earlier work [3–6] with both reinforced and unreinforced polycrystalline oxides and glasses, has shown that the ratio of densification to creep rate remains relatively constant from the beginning of densification to relative densities greater than 0.90. This indicates that the mechanism which leads to the reduction in densification rate is active from the very early stages of sintering.

An important factor during the simultaneous creep and densification of a porous compact is the influence of the pores on the creep rate. The stress intensification factor, ϕ , has been used to account for the effect of changing density (i.e. changing porosity) on the creep rate. It is defined as the ratio of the cross-sectional area of the specimen, A , to its actual load-bearing area, A_c , i.e. $\phi = A/A_c$. Beere [7, 8] calculated ϕ using a method which accounted for the pore/grain boundary geometry. Vieira and Brook [9] found that the functional dependence of the stress intensification factor could be expressed as

$$\phi \approx \exp(aP) \quad (1)$$

where a depends upon the equilibrium dihedral angle and P is the porosity expressed as a fraction. Rahaman and De Jonghe [5] found that ϕ for unreinforced ZnO could be described by Equation 1 with $a \approx 5$. This is

close to the value of $a \approx 6$ predicted by Beere's model for the observed dihedral angle of $\approx 120^{\circ}$. The reason for the deviation might be the idealized geometry of the model which assumed that the number of pores per grain remains constant during sintering. In addition, the model assumes that the porosity is located solely along the grain boundaries.

The addition of inclusions has been found to affect the shear viscosity of composite materials. Work by the present authors [10] has measured the creep (shear) viscosity of a soda–lime glass containing nickel inclusions of varying sizes. It was found that inclusion size did not affect the creep viscosity for volume fractions of inclusions < 10 vol %. However, above 10 vol % there was an inclusion size effect with the viscosity increasing significantly with decreasing inclusion size. The data indicated that interaction between inclusions might be responsible for the observed inclusion size effect.

Thus, it is apparent that the presence of inclusions can affect the sintering process through modification of the thermodynamic factors (e.g. sintering stress), the kinetic factors (e.g. viscosity), or both of these. Creep sintering experiments can elucidate the mechanisms by which these factors are affected. The results of an investigation of the effects of rigid inclusions upon the creep and densification of a model polycrystalline matrix (ZnO), are reported here. The creep viscosity, stress intensification factor and the ratio of the densification to creep rate of reinforced and unreinforced matrices were measured as functions of the inclusion size.

2. Experimental procedure

Zinc oxide powder (reagent grade, Mallinckrodt Inc., Paris, Kentucky) with an average particle size of ≈ 0.3 μm was used as the matrix phase, and unstabilized zirconium oxide (ZrO_2) with two average sizes (3 and 14 μm) was used as the inclusion phase.

Prior to incorporation into the matrix the zirconia powder was pre-sintered to 1600 °C for 10 h to densify any soft agglomerates. After cooling, the powder was lightly ground in an agate mortar and pestle. The zinc oxide powder was combined with sufficient zirconia to form composites containing 10 vol % inclusions. The mixture was ball milled for 2 h while dispersed in isopropanol in a polypropylene container using zirconia balls as the milling media. After drying, the mixture was lightly ground in an agate mortar and pestle and then calcined for 30 min at 200 °C. The unreinforced zinc oxide powder was subjected to the same processing treatment. The resulting powders were pressed in a uniaxial die to form green compacts (6 mm diameter by 6 mm) with a matrix relative density of 0.50 ± 0.02 .

Sintering was performed in a recording dilatometer (Theta Industries, Port Washington, NY) either freely (no applied load) or with an applied load of 9.8 N. This load is expected to cause measurable creep but with no change in densification rate [3]. The samples were heated to 1000 °C at a constant heating rate of 4°C min^{-1} . The mass and dimensions of the samples were measured before and after sintering to determine initial and final matrix relative densities. In a separate set of experiments, the creep sintering runs were terminated after fixed times and the axial and radial shrinkage were measured. A different sample was used for each run.

3. Results

Fig. 1 shows the data for the axial shrinkage, $\ln(L/L_0)$, versus temperature for the unreinforced ZnO and the ZnO with 10 vol % of 3 and 14 μm inclusions under a load of 9.8 N. (L is the instantaneous length and L_0 is the original length.) A load of 9.8 N represents an initial stress of ≈ 300 kPa upon the green compact. The reduction in cross-sectional area during densifica-

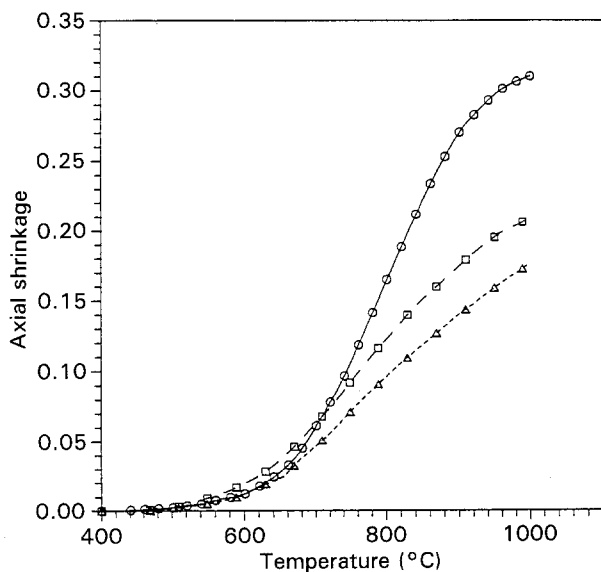


Figure 1 Axial shrinkage versus temperature for (○) unreinforced ZnO and composite samples containing 10 vol % ZrO₂ inclusions (△) 3 and (□) 14 μm in size. Sintered at 4°C min^{-1} to 1000 °C under an applied load of 9.8 N.

tion caused the stress to increase to ≈ 400 kPa at 1000 °C. Each curve is the average of two runs under the same conditions and the data are reproducible to $\pm 2\%$. As shown, the axial shrinkage begins at ≈ 600 °C and under identical conditions, the presence of the inclusions causes a reduction in the axial shrinkage. The magnitude of the reduction decreases with increasing inclusion size.

The radial strain was found to be a linear function of the axial strain i.e. $\epsilon_r = K\epsilon_z$ where K is a constant. These results are similar to those found by Rahaman and De Jonghe [3, 5] for pure ZnO and ZnO reinforced with 10 vol % SiC. The K values are shown in Table I. Similar experiments for free-sintered samples (i.e. sintered with no applied load) found that K was 0.98 (i.e. essentially isotropic shrinkage) for both the unreinforced ZnO and the composite samples [1].

Fig. 2 shows the matrix relative density versus temperature, calculated from the data of Fig. 1 and Table I, for the unreinforced ZnO and the composite samples. The results shown are the average of two experimental runs which vary by less than $\pm 2\%$. Note that the final matrix relative density decreases with decreasing inclusion size. For comparison, Fig. 3 taken from [1] shows the relative density versus temperature for freely sintered samples of unreinforced ZnO and ZnO matrix composites with 10 vol % of 3 and 14 μm inclusions. The samples were sintered at 4°C min^{-1} to 1200 °C. The densification of the samples begins at a higher temperature, ≈ 700 °C, and the densities at

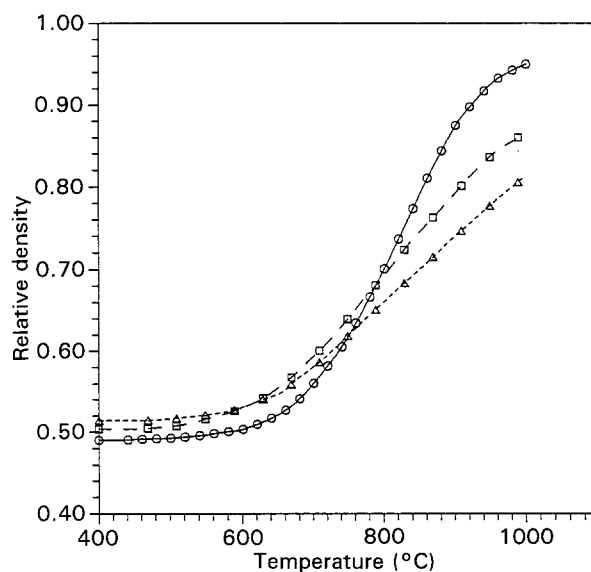


Figure 2 Matrix relative density versus temperature for samples shown in Fig. 1.

TABLE I Data for $K (= \epsilon_r/\epsilon_z)$ for ZnO matrix composites containing 10 vol % ZrO₂ inclusions sintered with an applied load of 300 kPa

Inclusion (vol %)	Size (μm)	K
0		0.62
10	14	0.70
10	3	0.75

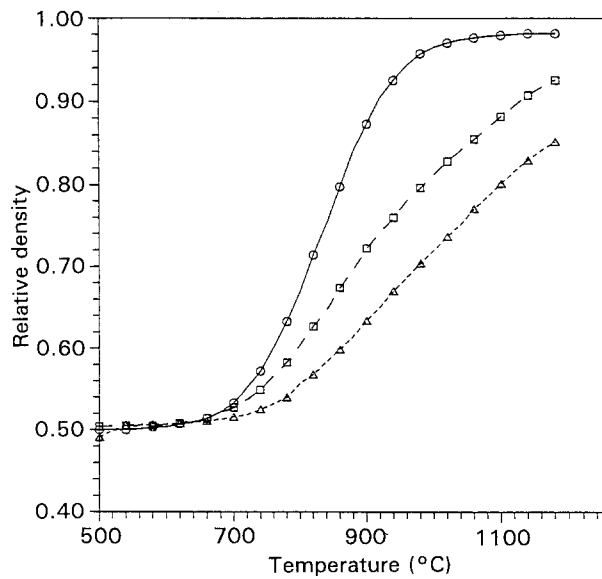


Figure 3 Relative density versus temperature for (○) unreinforced ZnO and composite samples containing 10 vol% ZrO_2 inclusions (△) 3 and (□) 14 μm in size. Free sintered at $4^\circ C \text{ min}^{-1}$ to $1200^\circ C$.

$1000^\circ C$ are lower compared to samples sintered with an applied load.

The axial strain rate, $\dot{\epsilon}_z$, was evaluated by fitting a smooth curve through the data points in Fig. 1, differentiating and multiplying by the heating rate. The creep strain rate, $\dot{\epsilon}_c$, and the densification rate, $\dot{\epsilon}_p$, were evaluated using equation [3]

$$\dot{\epsilon}_c = (2/3)(\dot{\epsilon}_z - \dot{\epsilon}_r) \quad (2)$$

$$\dot{\epsilon}_p = \dot{\rho}/\rho = -(\dot{\epsilon}_z + 2\dot{\epsilon}_r) \quad (3)$$

Because there is a linear relationship between ϵ_z and $\dot{\epsilon}_r$, Equations 2 and 3 can be rewritten

$$\dot{\epsilon}_c = (2/3)(1 - K)\dot{\epsilon}_z \quad (4)$$

$$\dot{\epsilon}_p = \dot{\rho}/\rho = -(1 + 2K)\dot{\epsilon}_z \quad (5)$$

Fig. 4 shows the densification rate versus temperature for the experimental results. The densification

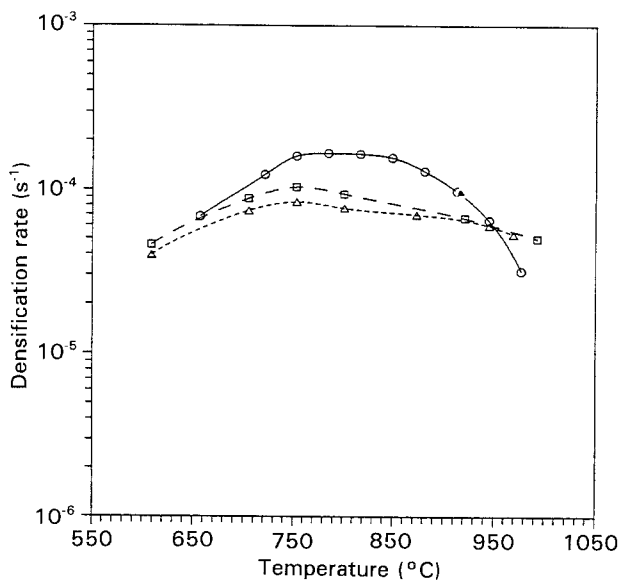


Figure 4 Densification rate for (○) unreinforced ZnO and composite samples containing 10 vol% ZrO_2 inclusions (△) 3 and (□) 14 μm in size versus temperature. Samples sintered under an applied load of 9.8 N.

rates of the composites remain relatively constant with temperature while the unreinforced ZnO exhibits a maximum at $\approx 800^\circ C$. The densification rates of the composites are comparable to or greater than those of the unreinforced ZnO above $\approx 920^\circ C$ indicating that the mechanisms that retard densification are relaxed at higher temperatures. Fig. 5 presents the same results for free-sintered samples. These are essentially the same as those in Fig. 4 indicating that the applied load does not affect the densification rate.

Fig. 6 is a plot of the creep rate versus temperature for the unreinforced ZnO and the composite samples. The creep rate for the composite samples is substantially less than that of the unreinforced ZnO. Comparison of Figs 4 and 6 indicates that the presence of the inclusions has a greater effect upon the creep rate

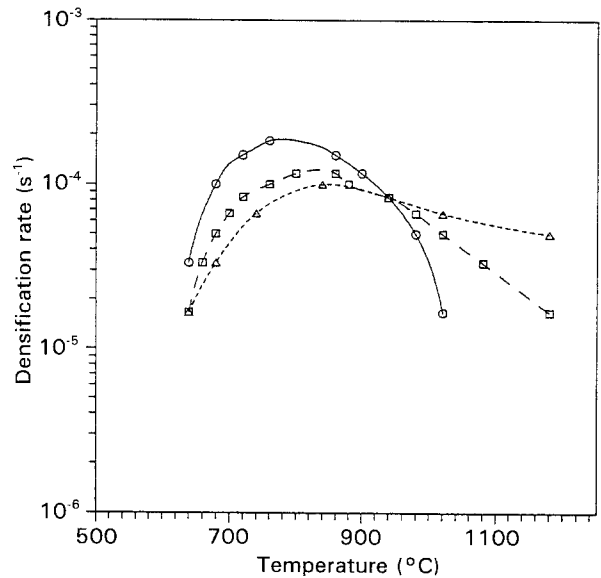


Figure 5 Densification rate for free-sintered samples of (○) unreinforced ZnO and composite samples containing 10 vol% ZrO_2 inclusions (△) 3 and (□) 14 μm in size versus temperature.

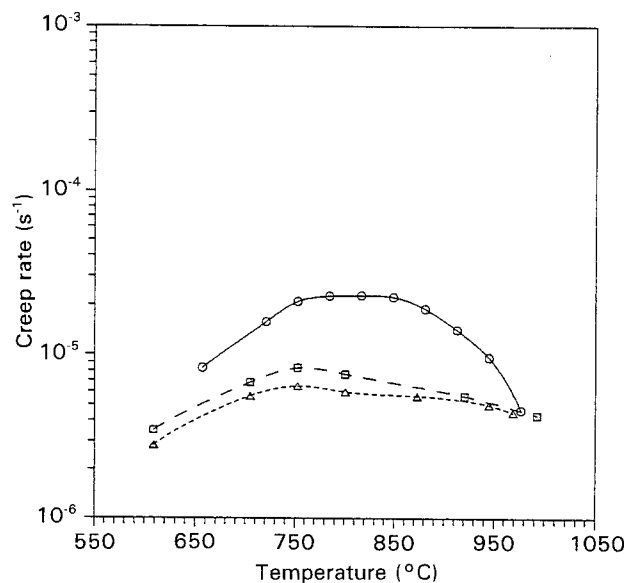


Figure 6 Creep rate for (○) unreinforced ZnO and composite samples containing 10 vol% ZrO_2 inclusions (△) 3 and (□) 14 μm in size versus temperature. Samples sintered under an applied load of 9.8 N.

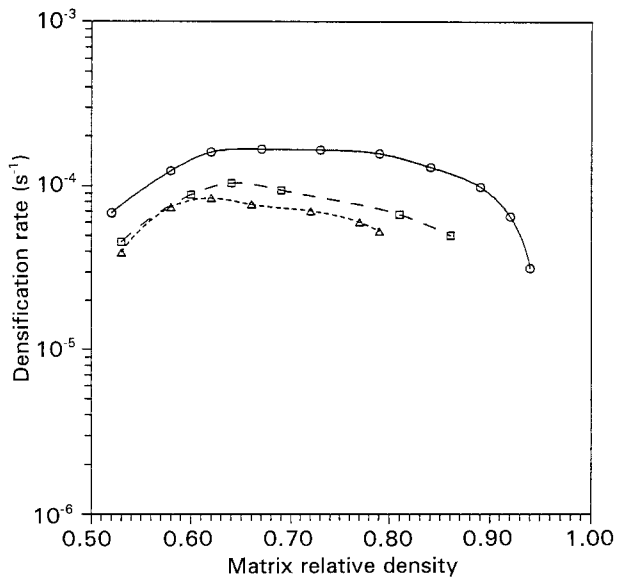


Figure 7 Densification rate for (○) unreinforced ZnO and composite samples containing 10 vol % ZrO₂ inclusions (△) 3 and (□) 14 μm in size versus matrix relative density. Samples sintered under an applied load of 9.8 N.

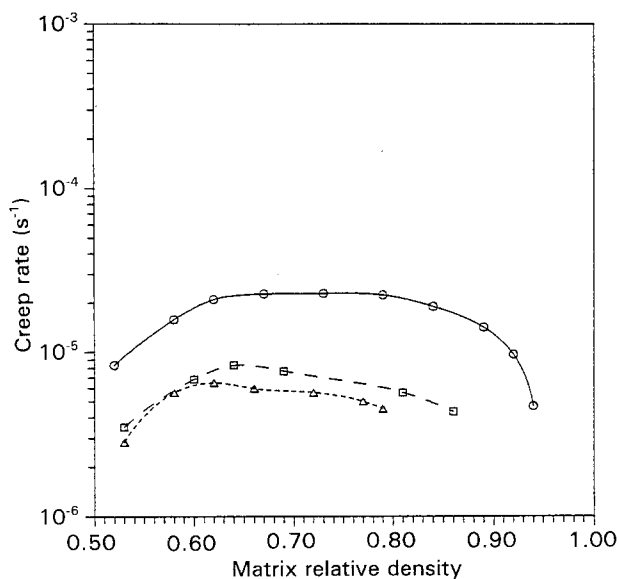


Figure 8 Creep rate for (○) unreinforced ZnO and composite samples containing 10 vol % ZrO₂ inclusions (△) 3 and (□) 14 μm in size versus matrix relative density. Samples sintered under an applied load of 9.8 N.

of the composite than upon the densification rate. There appears to be a slight inclusion size effect in that the creep and densification rates of the composite samples containing 3 μm inclusions are slightly lower than those containing 14 μm inclusions. Fig. 7 shows the densification rate and Fig. 8 the creep rate plotted against matrix relative density. The results show that the densification and creep rates of the composite samples are less than those of the unreinforced ZnO at any relative density. Figs 7 and 8 show that the presence of the inclusions affects the creep rate more than the densification rate.

4. Discussion

4.1. The creep viscosity

The creep viscosity of the porous compacts, η_c , was calculated from the creep rate, $\dot{\epsilon}_c$, and the applied

stress, σ_z , i.e. $\eta_c = \sigma_z / \dot{\epsilon}_c$. The applied stress was corrected for the changing cross-sectional area of the sample. The results are shown in Fig. 9 versus matrix relative density. The creep viscosity for the composite with 14 μm inclusions is approximately two to three times that of the unreinforced ZnO while the creep viscosity of the composite containing 3 μm inclusion is approximately four to five times that of the unreinforced matrix. The creep viscosity of the unreinforced ZnO remains relatively constant from relative densities ranging from 0.60–0.82 after which it increases rapidly during the last stages of sintering. The creep viscosity of the composite samples begins to increase at a lower relative density (0.60–0.65) which is an indication that the effect of the inclusions upon the creep viscosity (i.e. the creep rate) begins during the early stages of sintering.

The effect of rigid inclusions on sintering has been modelled by Scherer [11] using a self-consistent model developed by Budiansky [12]. In this model, the properties of the composite are found from the known properties of the inclusion and the matrix by deriving the properties of an effective medium made up of both. Another version of the self-consistent model developed by Christensen [13] can be used to predict the ratio of the composite creep viscosity to that of the unreinforced matrix. This model predicts that the inclusion phase will cause the creep viscosity to increase by approximately a factor of two and a half at a volume fraction of 10 vol %. As previously discussed by the present authors [10], theoretical predictions of the creep viscosity treat the matrix as a continuum. In addition, model predictions make no assumptions concerning inclusion size and assume that there is no contact between the inclusions within the matrix.

If the inclusion size is much greater than the matrix grain size, the polycrystalline matrix can reasonably be regarded as a continuum. For the composite samples used in these experiments, the initial ratio of

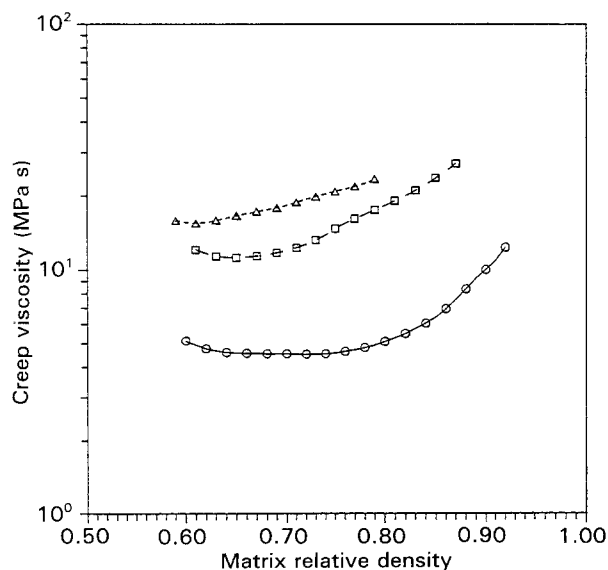


Figure 9 Creep viscosity versus matrix relative density for (○) unreinforced ZnO and composite samples containing 10 vol % ZrO₂ inclusions (△) 3 and (□) 14 μm in size.

inclusion diameter to the matrix grain size was ≈ 10 and ≈ 50 for the 3 and 14 μm inclusions, respectively. The magnitude of the increase in the measured creep viscosity due to the inclusions shown in Fig. 9 is comparable to that predicted by Christensen's self-consistent model. The slight size effect of the inclusions on the viscosity is most likely due to the difference in the ratio of the inclusion size to the initial matrix grain size of the 3 and 14 μm inclusions.

4.2. The stress intensification factor, ϕ

The creep data can be expressed in the form [3, 4]

$$\dot{\epsilon}_c = AD \phi(\rho) \sigma_z / (TG^m) \quad (6)$$

where A is a numerical constant, D is the diffusion coefficient, $D = D_0 \exp(-Q/RT)$ with Q equal to the activation energy, R is the gas constant, T is the absolute temperature and D_0 is a constant. The stress intensification factor $\phi(\rho)$, where ρ is the relative density ($\rho = 1 - P$), σ_z is the applied stress and G is the grain size at T , the absolute temperature. The exponent m is characteristic of the creep mechanism of the matrix material during sintering. Previous studies indicate that the sintering of ZnO involves mass transport by lattice diffusion (i.e. a Nabarro-Herring mechanism) for which $m = 2$ [15].

The stress intensification factor can be determined from

$$[\phi(\rho)]^{-1} = AD \sigma_z / (TG^m \dot{\epsilon}_c) \quad (7)$$

To determine the functional dependence of ϕ on density, the changes in D and G during sintering must be taken into account. Fig. 10, taken from Fan and Rahaman [1], shows the grain growth of unreinforced ZnO and composite samples containing 10 vol % ZrO_2 inclusions. The sintering was performed at a constant heating rate of 4°C min^{-1} to 1200°C . No grain growth occurred until the temperature reached

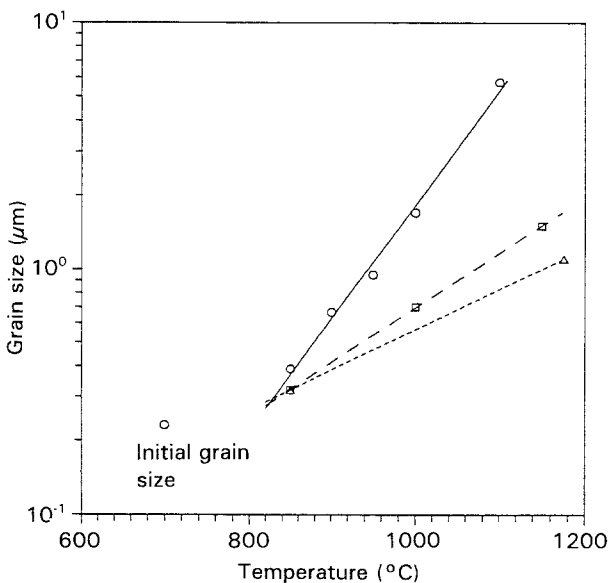


Figure 10 Matrix grain size versus temperature for (○) unreinforced ZnO and composite samples containing 10 vol % ZrO_2 inclusions (Δ) 3 and (\square) 14 μm in size during constant heating rate sintering.

$\approx 800^\circ\text{C}$. The slope of the line for the unreinforced ZnO indicates that the grain growth exponent is 3. Note that the inclusions reduce the rate of grain growth with the smaller 3 μm inclusions having the greatest effect. These results were used to compensate for the grain growth during sintering of both the unreinforced ZnO and the composite samples. The diffusion, D , was evaluated at each temperature, T , using an activation energy of 45 kcal which previous studies [16] indicate is a representative value for ZnO.

Fig. 11 is a plot of the stress intensification factor normalized by D_{600} and G_0 versus relative density. D_{600} is the diffusion term evaluated at 600°C which is the temperature when densification begins, and G_0 is the initial grain size, $\approx 0.3 \mu\text{m}$. This normalization shifts the curves vertically and does not affect the slope of the lines. The straight lines on the semi-log plot of Fig. 11 indicate that an exponential relation accurately describes both the unreinforced ZnO and the composite samples.

The slopes of the lines in Fig. 11 yield the constant a in Equation 1. The value of a for the unreinforced ZnO is ≈ 5 which is identical to the results obtained by Rahaman and De Jonghe [8]. The composite samples with 14 and 3 μm inclusions have a values of 11.3 and 13.0, respectively. Previous work by Rahaman and De Jonghe [3], presented the creep rates for isothermally sintered ZnO reinforced with 10 vol % SiC, but did not calculate a stress intensification exponent. Using their results and grain growth data from [1] it is possible to estimate a value for $a \approx 11$ which is comparable to the results presented here for ZnO reinforced with 10 vol % ZrO_2 .

The greater a values of the composite samples indicate that the stress intensification factor of the composites exhibit a stronger density dependence than the unreinforced ZnO. As previously mentioned, for the observed dihedral angle of $\approx 120^\circ$, the Beere model

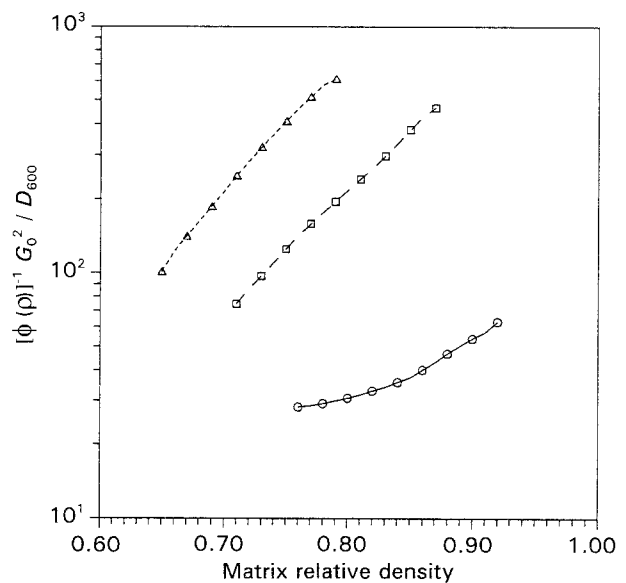


Figure 11 Stress intensification factor, $[\phi(\rho)]^{-1}$, versus matrix relative density for (○) unreinforced ZnO and composite samples containing 10 vol % ZrO_2 inclusions (Δ) 3 and (\square) 14 μm in size. Results have been normalized by D_{600} , the diffusion coefficient at 600°C , and G_0 , the initial grain size, $0.25 \mu\text{m}$.

predicts $a = 6$ which is reasonably close to the experimental value of 5. However, the a measured for the composite samples correlates to a dihedral angle of $\approx 50^\circ$ which is not reasonable considering both the low volume fraction of inclusions in the composite samples and that there is no reaction between the ZrO_2 and the matrix. This indicates that the assumptions of the Beere model may not be applicable to the composite samples investigated in this work.

Fig. 12 taken from [1] is a scanning electron micrograph of the polished surface of a composite containing 10 vol % inclusions ($14 \mu\text{m}$) after sintering to 1200°C at 4°C min^{-1} . The relative density of the composite matrix is 0.90. As can be seen, the porosity appears in two distinct regions: (i) immediately surrounding the inclusions, and (ii) within the bulk of the matrix. The porosity within the matrix is relatively uniformly distributed. The inclusions constrain the bulk of the matrix preventing it from densifying at the same rate as the unreinforced sample. As previously noted, the Beere model assumes that all porosity is distributed along the grain boundaries which is obviously not valid for the composite sample shown in Fig. 12. Although an exponential relation still appears to be valid, additional factors besides the dihedral angle, such as the packing of the matrix around the inclusion and possible inclusion-inclusion interactions, may be important considerations.

4.3. The ratio of densification rate to creep rate

Fig. 13 is a plot of the ratio of the densification rate to creep rate for the unreinforced ZnO and the composite samples, normalized to a stress of 300 kPa, versus matrix relative density. The ratios are essentially constant over a range of relative densities from 0.50–0.90. The composite samples have a ratio that is ≈ 1.5 times greater than that of the unreinforced ZnO regardless of inclusion size. Rahaman and De Jonghe [3] found similar results for isothermally sintered ZnO reinforced with 10 vol % SiC except that the composite ratio was only approximately one-half that of the unreinforced ZnO. While the results of the two

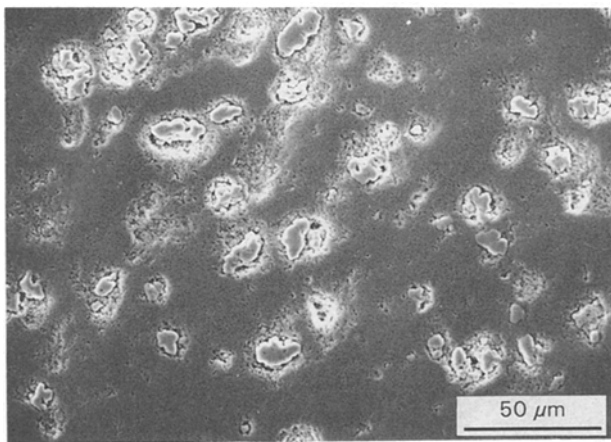


Figure 12 Scanning electron micrograph of the polished surface of a composite containing 10 vol % ZrO_2 inclusions ($14 \mu\text{m}$ in size) after sintering at 4°C min^{-1} to 1200°C .

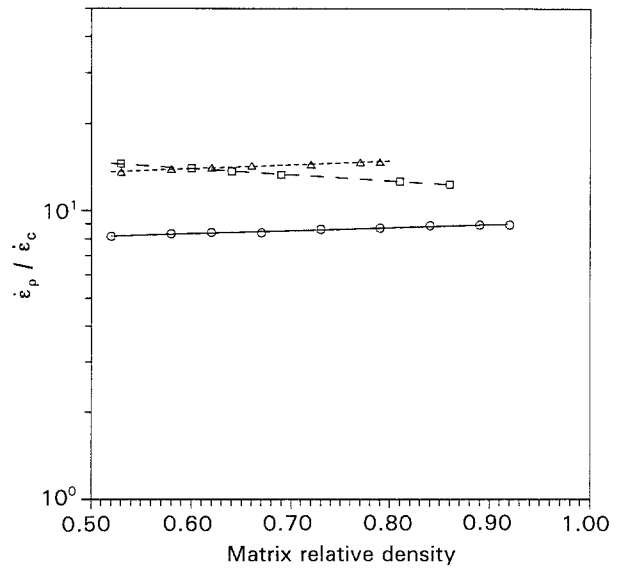


Figure 13 Ratio of densification rate to creep rate normalized to a stress of 300 kPa versus matrix relative density for (○) unreinforced ZnO and composite samples containing 10 vol % ZrO_2 inclusions (△) 3 and (□) $14 \mu\text{m}$ in size.

sets of experiments show that the inclusions affect the magnitude of the ratio differently, they indicate that the ratio of densification to creep rate is relatively constant versus time (e.g. isothermal sintering) and versus temperature (e.g. constant heating rate sintering).

To discuss the effects produced by the inclusions on the magnitude of the ratio, it is necessary to examine the various factors which can influence it. The creep and densification rates can be expressed as [4, 14]

$$\dot{\epsilon}_p \approx \Sigma \phi_p^{(m-1)/2} (\eta_c)^{-1} \quad (8)$$

$$\dot{\epsilon}_c \approx \sigma_a \phi_p^{(m-1)/2} \phi_c (\eta_p)^{-1} \quad (9)$$

where Σ is the sintering stress, σ_a is the applied uniaxial stress, and η_p is the densification viscosity, and separate stress intensification factors have been used for densification, ϕ_p , and creep, ϕ_c . The sintering stress is equivalent to an externally applied hydrostatic stress resulting in a densification rate that is equivalent to that caused by surface tension as the pore shrink. The ratio of the densification rate to creep rate is

$$\dot{\epsilon}_p / \dot{\epsilon}_c \approx (\Sigma / \sigma_a) (\eta_c / \eta_p) \phi_c^{-1} \quad (10)$$

As noted above, the experimental results given here and for the SiC-reinforced ZnO indicate that the ratio of densification to creep rate is constant. The factors that influence the creep and densification viscosities should be roughly comparable such that a change in one is likely accompanied by a similar change in the other. Hence, the ratio of the viscosities would be expected to remain relatively constant during sintering. The applied stress increases as the sample shrinks during densification and it is plausible to expect that the presence of the inclusions will cause the sintering stress to decrease with increasing density [3]. These factors would tend to reduce the ratio of the densification rate to the creep rate of the composites relative to that of the unreinforced matrix. This would explain

the results seen for the isothermally sintered composites containing SiC but not those of the constant heating rate sintered composites presented here.

In addition to employing isothermal sintering, the applied load used in the SiC composite experiments was 7 N. The current work used an applied load of 9.8 N which is 40% greater. Hence, the mechanisms which affect the creep rate may explain the differing results. The creep stress intensification factor is often thought to be equivalent to the densification stress intensification factor although this may not be strictly accurate [4]. As previously noted, the sintering stress associated with densification is equivalent to an externally applied hydrostatic stress resulting in a densification rate that is equivalent to that caused by surface tension as the pores shrink. Because it is a hydrostatic stress, no stress redistribution occurs during densification. For uniaxial creep this is not the case, because stress redistribution does occur due to such mechanisms as diffusion-controlled grain-boundary sliding. Hence the stress intensification factors for densification and creep are not strictly equivalent because the stress regimes are not equivalent. The stress intensification factors will be affected by the mechanisms that oppose creep and densification and also the rate at which they relax out as temperature increases.

Thus the reason for the differing results may be associated with the higher applied load and the behaviour of the creep stress intensification factor with temperature. However, it is not clear why the creep stress intensification factor of the composite should decrease more than that of the unreinforced matrix so that the ratio of the densification to creep rate of the composite becomes greater than that of the unreinforced matrix. Further experiments will be necessary to address this issue fully.

5. Conclusions

The creep and densification of unreinforced ZnO and composites containing 10 vol % ZrO₂ inclusions were investigated during constant heating rate sintering under an applied stress of ≈ 350 kPa. The presence of the inclusions decreased the creep rate to a greater extent than the densification rate but the ratio of the densification to creep rate remained constant with relative density.

The creep viscosity for the composite samples was approximately two to five times greater than that of the unreinforced matrix with the viscosity increasing with decreasing inclusion size. The increase in vis-

cosity was comparable to that predicted by a self-consistent model of the creep viscosity of a composite material.

The stress intensification factor for both the unreinforced ZnO and the composite samples was of the form $\phi \approx \exp(aP)$. The constant a was found to increase from 5 for the unreinforced matrix to ≈ 12 for the composite samples. Although the Beere model was reasonably accurate for the unreinforced ZnO, the model assumptions may not be appropriate for composite samples. In particular, the assumption that all porosity is located along the grain boundaries does not appear to be valid for the composite samples.

The ratio of the densification rate to creep rate for the composites was ≈ 1.5 times that of the unreinforced matrix regardless of inclusion size. This was different from the results seen for isothermally sintered ZnO containing 10 vol % SiC where the ratio of the composite sample was approximately one-half that of the unreinforced ZnO. The difference may be due to the different sintering techniques employed in each experiment.

Acknowledgements

This work was supported by the Air Force Office of Scientific Research under Grant 90-0267.

References

1. C. L. FAN and M. N. RAHAMAN, *J. Am. Ceram. Soc.* **75** (1992) 2056.
2. C. L. HU and M. N. RAHAMAN, *ibid.* **75** (1992) 2066.
3. M. N. RAHAMAN and L. C. DE JONGHE, *ibid.* **73** (1990) 602.
4. *Idem*, *Acta Metall.* **36** (1988) 223.
5. *Idem*, *J. Mater. Sci.* **22** (1987) 4326.
6. *Idem*, *J. Am. Ceram. Soc.* **70** (1987) C-348.
7. W. BEERE, *Acta Metall.* **23** (1975) 131.
8. *Idem*, *ibid.* **23** (1975) 139.
9. J. M. VIEIRA and R. J. BROOK, *J. Am. Ceram. Soc.* **67** (1984) 245.
10. R. E. DUTTON and M. N. RAHAMAN, *ibid.* **75** (1992) 2146.
11. G. W. SCHERER, *ibid.* **70** (1987) 719.
12. B. BUDIANSKY, *J. Mech. Phys. Solids* **13** (1965) 223.
13. R. M. CHRISTENSEN, *ibid.* **38** (1990) 379.
14. M. N. RAHAMAN, L. C. DE JONGHE and R. J. BROOK, *J. Am. Ceram. Soc.* **69** (1986) 53.
15. T. K. GUPTA and R. L. COBLE, *ibid.* **51** (1968) 521.
16. M.-Y. CHU, L. C. DE JONGHE and M. N. RAHAMAN, *Acta Metall.* **37** (1989) 1415.

Received 4 September 1992

and accepted 27 September 1993